R. SZEWCZYK*,#

### STRESS-INDUCED ANISOTROPY AND STRESS DEPENDENCE OF SATURATION MAGNETOSTRICTION IN THE JILES-ATHERTON-SABLIK MODEL OF THE MAGNETOELASTIC VILLARI EFFECT

The paper presents the results of the magnetoelastic Villari effect modelling in high-permeability $Mn_{0.51}Zn_{0.44}Fe_{2.05}O_4$ ferrite. Modelling was performed on the basis of measurements of magnetoelastic characteristics of frame-shaped samples. For the modelling, the corrected Jiles-Atherton-Sablik model was used. On the base of modelling results, the stress dependence of parameter k and stress-induced anisotropy were estimated. As a result the changes of saturation magnetostriction of $Mn_{0.51}Zn_{0.44}Fe_{2.05}O_4$ ferrite subjected to stresses were calculated. Such changes were previously observed experimentally. However, the phenomenon of stress-induced sign change of saturation magnetostriction was never previously explained quantitatively.

*Keywords*: magnetic hysteresis model, soft ferrite, magnetoelastic anisotropy

## 1. Introduction

The magnetoelastic Villari effect was described for the first time in 1865 by the Italian physicist E. Villari [1]. This effect is connected with the changes of flux density $B$ (achieved for a given value of the magnetizing field $H$) in the material subjected to mechanical stresses $\sigma$. The magnetoelastic Villari effect was observed in steel [2, 3, 4], soft ferrites [5] as well as amorphous [6, 7] and nanocrystalline [8, 9] soft magnetic materials.

In spite of the fact, that the magnetoelastic Villari effect is known for nearly 150 years, quantitative description of this effect for soft magnetic materials is still only partial. General tendencies of changes of flux density $B$ in material under stresses $\sigma$ are determined by the Le Chatelier's principle [10]. From the qualitative point of view it was experimentally proved that the way in which material responds to the influence of stresses $\sigma$ depends on the value of the product $\lambda_s\sigma$, where ls is the saturation magnetostriction. Note that tensile and compressive stresses $\sigma$ are considered positive and negative respectively. If the value of this product is significantly negative, the decrease of flux density $B$ under stresses $\sigma$ is observed. On the other hand, for positive value of product lsσ, the increase of flux density $B$ was observed, up to the maximum, called magnetoelastic Villari point [11]. It should be indicated, that quantitative explanation of appearance of the magnetoelastic Villari point on $B(\sigma)$ characteristics was not presented previously.

The most advanced quantitative descriptions of magnetoelastic Villari effect were given by Armstrong model [12, 13], ΔE-based models [14] and Jiles-Atherton-Sablik model [15, 16, 17]. However, the Jiles-Atherton model was developed for isotropic materials [18, 19], whereas the presence of mechanical stresses generates significant stress-induced anisotropy $K_\sigma$ in the material. This stress-induced anisotropy created in the isotropic material was not considered in the original Jiles-Atherton-Sablik model. Filling this gap will create possibility of more accurate modelling of influence of mechanical stresses on the shape of magnetic hysteresis loop. Moreover, it will create possibility of numerical determination of experimentally observed [20] changes of saturation magnetostriction $\lambda_s$ of magnetic material subjected to mechanical stresses $\sigma$.

## 2. Principles of the Jiles-Atherton-Sablik model

The Jiles-Atherton-Sablik model of magnetomechanical effect is based on analysis of total free energy of a magnetic material. In this model, effective magnetization field $H_e$ in the material subjected to mechanical stresses σ generated in the direction of the magnetizing field H is given by the following equation [21]:

$$H_e = H + \alpha M + \frac{3\sigma}{2\mu_0}\left(\frac{\partial \lambda}{\partial M}\right) \tag{1}$$

where $M$ is the magnetization of the magnetic material and m0 is the magnetic constant. Magnetization dependence of magnetostriction in the magnetic material $\lambda(M)$ covers magnetostrictive hysteresis and lift-off phenomenon [22]. However, experimental results indicate that for high-permeability ferrites these phenomena may be neglected [23] and $\lambda(M)$ can be estimated by quadratic equation:

$$\lambda(M) = \frac{3\lambda_s}{2M_s^2}M^2 \tag{2}$$

* WARSAW UNIVERSITY OF TECHNOLOGY, INSTITUTE OF METROLOGY AND BIOMEDICAL ENGINEERING, 8 ŚW. A. BOBOLI STR., 02-525 WARSZAWA, POLAND

# Corresponding author: rszewczyk@onet.pl

608

where $M_s$ is the saturation magnetization of a magnetic material. On the basis of equations (1) and (2), the effective magnetization field $H_e$ may be calculated as [21]:

$$H_e = H + \alpha M + \frac{9\sigma\lambda_s}{2\mu_0 M_s^2}M = H + \hat{\alpha}M \qquad (3)$$

where the stress-sensitive parameter $\hat{\alpha} = \alpha + \frac{9\sigma\lambda_s}{2\mu_0 M_s^2}$.

The Jiles-Atherton-Sablik model is based on the anhysteretic magnetization curve $M_{ah}(H_e)$. In a general case, for anisotropic materials, this curve given by the equation [24, 25]:

$$M_{ah} = M_s \left[ \frac{\int_0^\pi e^{0.5(E(1)+E(2))} sin\theta \cdot cos\theta \cdot d\theta}{\int_0^\pi e^{0.5(E(1)+E(2))} sin\theta \cdot d\theta} \right] \qquad (4)$$

where $\theta$ is the integration parameter and $E(i)$, is given by the following relationship [24]:

$$E(i) = \frac{H_e}{a} cos\theta - \frac{K_{an}}{M_s \cdot \mu_0 \cdot a} sin^2 \phi_i \qquad (5)$$

where $a$ quantifies domain wall density, $K_{an}$ is the anisotropic energy density, $\phi 1 = \psi - \theta$ and $\phi 2 = \psi + \theta$, where $\psi$ is an angle between the easy axis of the material and the magnetizing field direction.

It should be indicated, that in the case of anhysteretic magnetization of the isotropic magnetic materials $M_{an}$, where $K_{an}=0$, equation (4) reduces to the Langevin equation [15]:

$$M_{an} = M_{ah}\big|_{Kan=0} = M_s \left[ coth\left(\frac{H_e}{a}\right) - \left(\frac{a}{H_e}\right) \right] \qquad (6)$$

For isotropic materials integral in equation (4) has the antiderivative. As a result it can be reduced to the Langevin function in equation (6). However, for other values of $K_{an}$, anhysteretic value of the magnetisation $M_{ah}$ can be calculated only using numerical methods.

In the original Jiles-Atherton-Sablik model, the total value of anhysteretic magnetization is calculated as a weighted sum of isotropic and anisotropic magnetisation [26]. This assumption is correct in the case of some magnetic materials with anisotropy induced during production processes, such us cold rolled electrical steels. However, in the case of isotropic materials with stress-induced anisotropy, consideration of isotropic phase in anisotropic materials is not necessary.

In the Jiles-Atherton-Sablik model, total magnetization in the material is given as a sum of reversible magnetization Mrev and irreversible magnetization Mirr [16]:

$$M = M_{rev} + M_{irr} \qquad (7)$$

Reversible magnetization $M_{rev}$ in the Jiles-Atherton-Sablik model can be calculated from the following equation [16]:

$$M_{rev} = c \cdot (M_{an} - M) \qquad (8)$$

where the parameter $c$ describes magnetization reversibility and is connected with the Globus model [16], where it is determined by the average surface energy of the domain wall.

An important part of the Jiles-Atherton-Sablik model is the irreversible magnetization $M_{irr}$ given by the differential equation [16]:

$$\frac{dM_{irr}}{dH_e} = \delta_M \frac{M_{an} - M}{\delta \cdot k} \qquad (9)$$

where the parameter $\delta$ is connected with changes of the magnetizing field H and is equal to +1 and -1 for $\frac{dH}{dt} \geq 0$ and $\frac{dH}{dt} < 0$ respectively. The parameter k of this model quantifies average energy required to break the pining site, and in the original Jiles-Atherton-Sablik model it is considered as a constant for a given sample of the magnetic material.

The parameter $\delta_M$ is necessary for avoidance of unphysical stages of the Jiles-Atherton-Sablik model for minor loops, where incremental susceptibility often becomes negative [27, 28]. This parameter is equal to 0 either when $\frac{dH}{dt} < 0$ and $M_{an} - M > 0$, or when $\frac{dH}{dt} \geq 0$ and $M_{an} - M < 0$. In the other cases $\delta_M = 1$ and can be neglected.

Finally, the total flux density $B$ in the magnetic material is equal to $M \times \mu_0$.

From the practical point of view, total magnetization M in the material may be calculated from the following equation [13]:

$$\frac{dM}{dH} = \frac{\delta_M}{(1+c)} \frac{(M_{an} - M)}{(\delta k - \hat{\alpha}(M_{an} - M))} + \frac{c}{(1+c)} \frac{dM_{an}}{dH} \qquad (10)$$

which is the result of differential forms of equations (7) and (8) together with equation (9). It should be noted that , that in equation (10) the irreversible magnetization $M_{irr}$ is reduced and does not have to be calculated separately to obtain the total magnetization $M$ in the magnetic material.

## 3. Proposed extension of the Jiles-Atherton-Sablik model by considering the stress-induced anisotropy

In the original Jiles-Atherton-Sablik model, mechanical stresses $\sigma$ affect the shape of $M(H)$ hysteresis loop only through effective magnetizing field $H_e$ (equation (1)). However, in the magnetic sample subjected to mechanical stresses $\sigma$, the stress-induced anisotropy $K_\sigma$ occurs. Energy density of the stress induced anisotropy $K_\sigma$ for given mechanical stresses $\sigma$ (oriented parallel to the magnetizing field $H$) is given by the following equation [10]:

$$K_\sigma = \frac{3}{2}\lambda_s \sigma \qquad (11)$$

As a result, even isotropic magnetic materials such as high-permeability Mn-Zn ferrites, subjected to mechanical stresses became anisotropic. For this reason, the anhysteretic magnetisation of such materials subjected to mechanical stresses cannot be calculated from Langevin equation (6). It should be calculated from equation (4) suitable for magnetic materials with the given anisotropy energy density $K_{an} = K_\sigma$.

It should be indicated that for the stress dependence modelling of the hysteresis loop $B(H)$, direct determination of the stress-induced anisotropy $K_\sigma$ is not necessary. Both the stress-induced anisotropy $K_s$ and changes of the effective

magnetizing field $H_e$ are determined by the stress dependence of saturation magnetostriction $\lambda_s(\sigma)$. As a result, the knowledge of $\lambda_s(\sigma)$ characteristic is sufficient for modelling the stress dependence of the magnetic hysteresis loop of isotropic materials, such as Mn-Zn ferrites. On the other hand, as far as the proposed extension of the Jiles-Atherton-Sablik model is concerned, the stress dependence of saturation magnetostriction $\lambda_s(\sigma)$ can be determined on the basis of the series of $B(H)$ magnetic hysteresis loops measured for different values of stresses $\sigma$.

## 4. Method of experiment

During the experiment the influence of compressive stresses $\sigma$ on the shape of hysteresis loops of the $Mn_{0.51}Zn_{0.44}Fe_{2.05}O_4$ ferrite was tested. Frame-shaped cores were used for the experiment. The compressive stress was applied to the columns of the frame-shaped core by the oil press. A schematic block diagram of the mechanical system for testing magnetoelastic properties of frame-shaped samples is presented in figure 1. Compressive stresses $F$ are applied to the frame-shaped sample (1) by non-magnetic backings (5) and ball-joints (6). It should be highlighted that uniform compressive stresses generated in the columns of the frame-shaped core are in line with direction of the magnetizing field $H$ [29]. Due to the fact, that $Mn_{0.51}Zn_{0.44}Fe_{2.05}O_4$ ferrite is a ceramic material, under compressive stresses of magnitudes up to 15 MPa no plastic deformation was observed. The hysteresis under stresses was measured using digitally controlled hysteresis graph for the frequency of the magnetizing field strength equal to 0.1 Hz. Details of this method of measurements of magnetoelastic properties of frame-shaped ferrite cores were presented previously [29, 30].
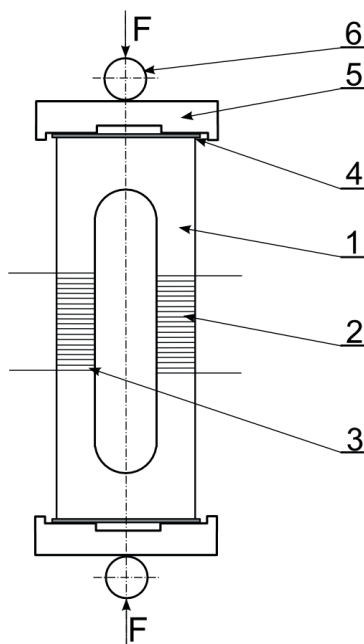
Figure 2 presents the influence of compressive stresses $\sigma$ on the shape of the $B(H)$ hysteresis loop. It should be indicated that compressive stresses $\sigma$ exhibit significant influence on both coercive force and on maximal flux density in the core [29, 30].



Fig. 2. The influence of compressive stresses on the shape of magnetic $B(H)$ hysteresis loops for the $Mn_{0.51}Zn_{0.44}Fe_{2.05}O_4$ ferrite

Figure 3 presents $B(\sigma)Hm$ magnetoelastic characteristics. These characteristics indicate the value of maximal flux density $B$ in materials subjected to stresses $\sigma$ achieved for a given value of amplitude of the magnetizing field $Hm$. It should be noted, that value of the flux density $B$ under compressive stresses $\sigma$ first increases and then decreases. Maximum of the $B(\sigma)$ $Hm$ characteristics is known as the Villari point or the Villari reversal. In the case of $Mn_{0.51}Zn_{0.44}Fe_{2.05}O_4$ ferrite, the Villari reversal was observed for compressive stresses of about 1.5 MPa.
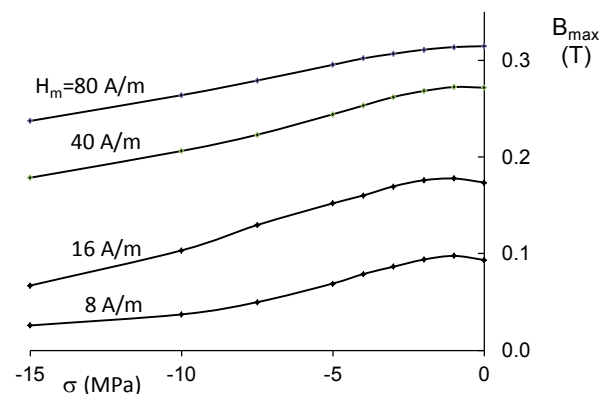


Fig. 3. Compressive stress $\sigma$ dependence of the maximal flux density $B_{max}$ achieved in the core for a given amplitude of the magnetizing field strength $H_m$

## 5. Method of modelling

According to the Jiles-Atherton-Sablik model, the magnetic hysteresis loop $M(H)$ can be calculated from equation (10). However, previously presented methods [31, 32] of solving of equation (10) with simple assumption of the small time step Dt may be risky due to the accumulation of numerical errors. As a result, in such case the value of numerical errors



Fig 1. Schematic block diagram of the system for testing the magnetoelastic properties of frame-shaped samples: 1 – sample under investigation, 2 – magnetizing winding, 3 – detection winding, 4 – elastic spacer, 5 – non-magnetic backing, 6 – ball joint, F – applied compressive force

during solving of equation (10) has to be carefully observed.

The most accurate solution of equation (10) may be given by the adaptive sampling explicit Runge-Kutta (2,3) pair of Bogacki and Shampine method [33] with relative numerical error lower than $10^{-4}$. This method is implemented in MATLAB and open-source OCTAVE with "odepkg" package as the "ode23" ordinary differential equation solver. However, in such a case, long time of calculation may be a problem, if parameters of the Jiles-Atherton-Sablik model are near its instability region [34]. Then, the fixed step fourth-order Runge-Kutta method for solving equation (10) is more calculation-time effective and generates relatively small numerical errors.

Numerical integration of equation (4) by the trapezoid method is calculation time effective and generates moderate numerical errors. However, to guarantee the required accuracy level (such as relative error lower than 10-8), the adaptive Gauss-Kronrod quadrature [35] should be used. This method is implemented in both MATLAB and OCTAVE as a "quadgk" numerical integration function.

Solution of equation (10) requires also numerical differentiation of $\frac{dM_{ah}}{dH}$. For this numerical differentiation the spline extrapolation to zero of the series of gradients was used.

Previously, there were presented different methods of direct determination of the Jiles-Atherton-Sablik model parameters [36, 37]. However, from the practical point of view, determination of the Jiles-Atherton-Sablik model parameters requires optimisation process. In this process the parameters are determined on the basis of minimisation of the following target function:

$$F = \sum_{i=1}^{n}\big(B_{model}(H_i) - B_{meas}(H_i)\big)^2 \qquad (12)$$

where $B_{model}(H_i)$ were the results of the modelling, and $B_{meas}(H_i)$ were the results of the measurements, both for the same $H_i$ value of the magnetizing field. The target function $F$ was calculated simultaneously for 4 hysteresis loops measured for different values of the magnetizing field amplitude. As a result, optimisation focused on finding the model parameters representing wide range of the magnetizing fields.

Presented simulations were made in the following three steps.

In the first step, the evolutionary strategies $(\mu+\lambda)$ [38] were used to determine five Jiles-Atherton-Sablik model parameters ($a, k, c, M_s, \alpha$) required for isotropic materials not subjected to stresses ($K_{an} = 0$). To increase the speed of calculations, this step was carried out with reduced numerical accuracy. In this case, fixed-step fourth-order Runge-Kutta method (50 steps) was used for solving differential equation (10), as well as 90 fixed-step trapezoid method was used for integration of equation (4).

In the second step, 20 best solutions of the evolutionary strategy was subjected to the Nelder-Mead simplex optimisation method [39] implemented in both MATLAB and OCTAVE as a "fminsearch" function. The best solution was chosen as a result of this step. To enhance the accuracy in this and the next step, the adaptive sampling explicit Runge-Kutta (2,3) pair of Bogacki and Shampine method was used for solving equation (10) together with adaptive Gauss-Kronrod quadrature for solving equation (4).

Finally in the third step, stress dependence of saturation magnetostriction $\lambda_s(\sigma)$ was calculated on the basis of experimental results. In this step, parameters $a, k, c, M_s$ were the same as for the stress-free sample. However, influence of stresses was incorporated by consideration of the effective magnetizing field He stress dependence, and the anhysteretic magnetization $K_{an} = K_{\sigma} = \frac{3}{2}\lambda_s\sigma$, influencing the results of modelling by equations (1) and (4) together with (11). It should be indicated that calculations in this step were also made simultaneously for 4 hysteresis loops measured for different magnetizing field amplitudes.

## 6. Results

During modelling the following parameters of the Jiles-Atherton-Sablik model were determined for the unstressed sample: $a = 7.402$ A/m, $c = 0.6308$, $M_s = 2.704\cdot10^5$ A/m, $\alpha = 1.411\cdot10^{-13}$. These parameters were considered not sensitive to compressive stresses.

Figure 4 presents the value of $R^2$ coefficient of determination calculated for results of measurements of hysteresis loops and the results of simulation. It can be observed that the quality of modelling decreases for higher values of compressive stresses. This is caused by the fact that for higher value of stresses, stress-induced changes of the shape of hysteresis loop are caused also by phenomena not connected with stress-induced anisotropy and changes of the energy required to break the pinning site, which are not taken into account by the values of parameters $K_{an}$ and $k$ of the model.
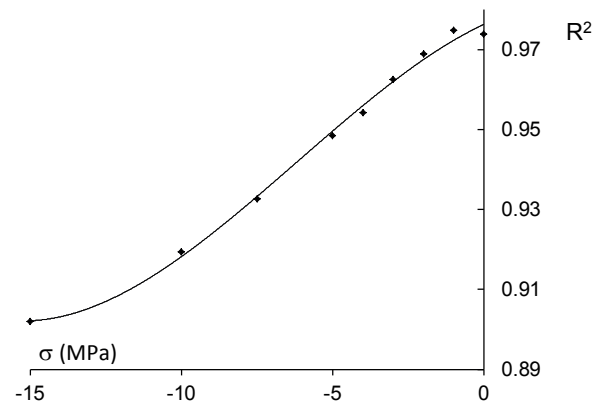


Fig. 4. Compressive stress $\sigma$ dependence of quality of modelling using the Jiles-Atherton-Sablik model described by $R^2$ determination coefficient

Figure 5a presents the results of modelling the compressive stress-induced changes of the average anisotropy energy density $K_{an}$, whereas figure 5b presents changes of the parameter $k$ under these stresses. It should be indicated that the average anisotropy energy density $K_{an}$ first increases under compressive stresses, and then, near the Villari point, it starts to decrease. On the other hand, value of the parameter $k$, describing in the model the average energy required to break the pinning site, monotonically increases under the compressive stresses. This effect is caused by the fact that mechanical stress increases the number of dislocations in the

crystalline materials which leads to increase of energy required to start domain wall movement (break the pining site).
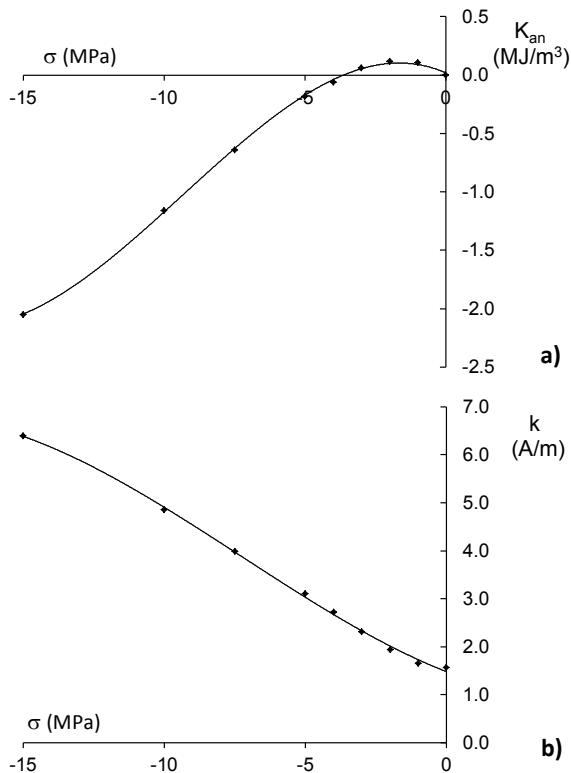


Fig. 5. Results of calculation of the compressive stresses $\sigma$ dependence of the Jiles-Atherton-Sablik model parameters: (a) average anisotropy energy density $K_{an}$, (b) parameter $k$ describing energy required to break the pinning site.

Figure 6 presents the results of calculation of changes of saturation magnetostriction ls in the material subjected to compressive stresses $\sigma$. For these calculations, the equation (11) was used. It may be observed that negative saturation magnetostriction increases under compressive stresses to change its sign near the Villari point. For higher values of compressive stresses, saturation magnetostriction ls of the $Mn_{0.51}Zn_{0.44}Fe_{2.05}O_4$ ferrite is positive. The phenomenon of sign change of magnetostriction was previously observed experimentally [20], but was never modelled quantitatively. Moreover, the extrapolated value of saturation magnetostriction 0.1 mm/m for unstressed material is in accordance with typical values measured experimentally for high-permeability Mn-Zn ferrites.
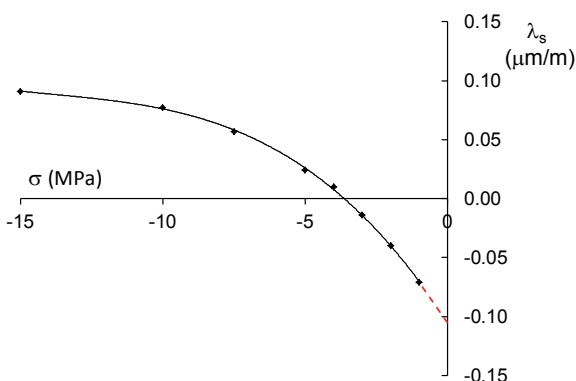


Fig. 6. Results of calculation of the compressive stresses $\sigma$ dependence

of saturation magnetostriction ls in the $Mn_{0.51}Zn_{0.44}Fe_{2.05}O_4$ ferrite calculated on the base of the Jiles-Atherton-Sablik model

## 7. Conclusions

Presented results confirm that mechanical stresses have significant influence on the shape of hysteresis loop of isotropic magnetic materials, such as the high-permeability $Mn_{0.51}Zn_{0.44}Fe_{2.05}O_4$ ferrite. In the Jiles-Atherton-Sablik model this influence may be explained by considering the stress-induced anisotropy as well as stress dependence of the parameter $k$ describing the average energy required to break the pinning site in the magnetic material.

Moreover, on the basis of quantitative analysis of stress dependence of the magnetic hysteresis loop, the value of stress-induced anisotropy for the given value of mechanical stresses may be estimated. This estimation creates the novel possibility of modelling the stress dependence of saturation magnetostriction $\lambda_s$ of magnetic materials. Such stress dependence was observed during the measurement, however it was previously not explained and not modelled qualitatively.

## REFERENCES

[1]  E. Villari, Annu. Rev. Phys. Chem. **126,** 87 (1865).

[2]  K. Kashiwaya, Jpn. J. Appl. Phys. **30,** 2932 (1991).

[3]  H.C. Rhim, B. H. Oh, H. S. Park, Key Eng. Mat. **377,** 321-323, (2006).

[4]  D. Jackiewicz, R. Szewczyk, J. Salach, A. Bieńkowski, M. Kachniarz, Advances in Intelligent Systems and Computing **267**, 607 (2014).

[5]  A. Bieńkowski, J. Kulikowski, J. Magn. Magn. Mater. **19**, 120 (1980).

[6]  L. Kraus, F. Fendrych, P. Švec, J. Bydžovský, M. Kollár, J. Optoelectron. Adv. M. **4**, 237 (2002).

[7]  A. Bienkowski, R. Szewczyk, R. Kolano, Materials Science and Engineering A-Structural Materials Properties Microstructure and Processing **375**, 1024 (2004).

[8]  G. Bordin, G. Buttino, A. Cecchetti, M. Poppi, J. Magn. Magn. Mater. **150**, 363 (1995).

[9]  R. Szewczyk, A. Bienkowski, J. Salach, E. Fazakas, L. K. Varga, J. Optoelectron. Adv. M. 5, 705 (2003).

[10]  B.D. Culity, Introduction to magnetic materials, 1972 Addison Wesley.

[11]  A. Bieńkowski, J. Magn. Magn. Mater. **231**, 215–216, (2000).

[12]  W. D. Armstrong, J. Appl. Phys. **81**, 2321 (1997).

[13]  C. Mudivarthi, S. Datta, J. Atulasimha, A. B. Flatau, Vtt. Symp. **17**, 035005 (2008).

[14]  B. Bergmair, T. Huber, F. Bruckner, C. Vogler, M. Fuger, D. Suess, J. Appl. Phys. **115,** 023905 (2014).

[15]  D. Jiles, D. Atherton, J. Magn. Magn. Mater. **61**, 48 (1986).

[16]  D.C. Jiles, J. Appl. Phys. **28**, 1537 (1995).

[17]  M. Sablik, D.C. Jiles, IEEE. T. Magn. **29**, 2113 (1993).

[18]  M.J. Dapino, R.C. Smith, A.B. Flatau, IEEE. T. Magn. **36**, 545 (2000).

[19]  M. J. Dapino, R.C. Smith, L.E. Faidley, A. B. Flatau, Journal of Intelligent Material Systems and Structures **11**, 135 (2000).

[20]  A. Bieńkowski, J. Kulikowski, J. Magn. Magn. Mater. **101**,

122 (1991).

[21] M. J. Sablik, H. Kwun, G. L. Burkhardt, D. C. Jiles, J. Appl. Phys. **61**, 3799 (1987).

[22] D.C. Jiles, J. Phys. D Appl. Phys. **28**, 1537 (1995).

[23] R. Szewczyk, PRAMANA-J. Phys. **67**, 1165 (2006).

[24] A. Ramesh, D.C. Jiles, J.M. Roderick, IEEE. T. Magn. **32**, 4234 (1996).

[25] R. Szewczyk. Materials **7**, 5109 (2014).

[26] D.C. Jiles, A. Ramesh, Y. Shi, X. Fang , IEEE. T. Magn. **33**, 3961 (1997).

[27] J.H.B. Deane, IEEE. T. Magn. **30**, 2795 (1994).

[28] K. Chwastek, J. Szczygłowski, Math. Comput. Simulat. **71,** 206 (2006).

[29] A. Bienkowski, J. Kulikowski, Acta Phys. Pol. A **72,** 303 (1987).

[30] A. Bienkowski, J. Magn. Magn. Mater. **101**, 125 (1991).

[31] F.T. Calkins, R.C. Smith, A.B. Flatau, IEEE. T. Magn. **36**, 429 (2000).

[32] R. Szewczyk, J. Phys. D Appl. Phys. **40**, 4109 (2007).

[33] P. Bogacki, L.F. Shampine, Appl. Math. Lett. **2**, 1 (1989).

[34] R. Szewczyk, Advances in Intelligent Systems and Computing **267**, 275 (2014).

[35] L.F. Shampine, J. Comput. Appl. Math. **211**, 131 (2008).

[36] K. Chwastek, J. Szczyglowski, Electrical Review **84**, 145 (2008).

[37] N. Pop, O. Caltun, Can. J. Phys. **89,** 787 (2011).

[38] H.P. Schwefel, Evolution and optimum seeking, 1995 Wiley.

[39] J.C. Lagarias, J. A. Reeds, M. H. Wright, P. E. Wright, SIAM J. Optimiz. **9**, 112 (1998).